

# A Review of Numerical Investigations Regarding the Supercritical Fluid Expansion in the RESS Process

Ali Ben Moussa and Hatem Ksibi

Sfax University, IPEIS, P. Box 1172, Sfax 3018 Tunisia

ali.benmoussa@ipeis.rnu.tn

hatem.ksibi@ipeis.rnu.tn

## ABSTRACT

In this work we undertake a comparative study of mathematical models and related (CFD) simulations for the so-called RESS process (rapid expansion of supercritical solutions), which so much attention has attracted in the literature for the potential applications related to the production of microparticulates of selected materials with controllable morphology and narrow-size distributions using supercritical fluids. The numerical computation of supercritical fluid flows, in general, is extremely challenging because of the complexity of the physical processes involved and the different space and time scales. The aim of this study is the focused analysis of advanced mathematical modeling of the supercritical fluid expansion in the RESS process with the specific intent of delineating a possible strategy for optimizing operating parameters. Particularly, the research goals are to examine numerically, influences of temperature, pressure, composition, flow rate and reactor dimensions on the fluid hydrodynamic to undertake study of transport and growth of the recrystallized particles.

**Keywords:** Numerical Simulation, Expansion, Supercritical Fluid, RESS Process, Shock Waves.

## 1. INTRODUCTION

The use of supercritical fluids (SCFs) is one of the most promising alternatives towards a “sustainable” chemistry. Supercritical CO<sub>2</sub> (or other supercritical fluids) are an environmentally benign alternative to conventional industrial solvents. Among others, they offer the possibility to reduce the size of reactor volumes to a great extent, and to accelerate chemical processes. In particular, the rapid expansion of supercritical solutions (RESS process) allows the production of powders with a narrow particle size distribution that is very important for applications in several industrial branches. The RESS process constitutes a new route to obtain finely divided solids which are of interest in many industrial applications, such as pharmaceutical aerosols, inks, pigments, and filtration media. The use of supercritical fluids for the formation of fine particles is receiving increased attention as a possible alternative to grinding and spray-drying with liquid solvents.

Micronization by dense gases is a convenient method because of the relative simplicity by which the properties can be manipulated by temperature and pressure. A supercritical fluid such as carbon dioxide with a moderate critical temperature of 31.2°C is commonly used as a dense gas. The process, therefore, performs at a moderate temperature, which is suitable for many heat labile compounds such as proteins and biocompatible polymers. In the supercritical fluid, the density and hence, solvent power of SCFs can be varied widely with small changes in the temperature and pressure around the critical region, enabling the use of SCFs as solvents or anti solvents during particle formation.

There are many published works in literature which are concentrated on both the simulation of supercritical fluid expansion and nucleation of the solute inside the nozzle capillary. Nevertheless, none among them have considered the fluid expansion beyond the nozzle as a free jet in a low pressure chamber. In recent studies, the hydrodynamics of supercritical expansion of carbon dioxide has been studied as a function of the nozzle geometry and the initial thermodynamics conditions.

In this paper, we give an overview of recent publications on the subject. Different models are detailed by giving related hypotheses and computational domains. Significant results are selected and

discussed to elaborate quite an exhaustive scenario about the influence of inlet/outlet operating parameters on the expansion of the supercritical fluid through different nozzle types.

## 2. HYDRODYNAMIC DESCRIPTION OF THE EXPANSION

### 2.1 RESS Principle

The RESS is a method of particle formation, recrystallization and particle size reduction as well as powder mixing. In this process, the solute is first dissolved in a SCF, which is then subjected to rapid expansion by passing it through a nozzle at supersonic velocities, figure (1).

During the expansion, an extremely fast phase change from the supercritical to the gas-like state takes place. The density and the solvation power of the SCF decrease dramatically, resulting in a high degree of solute supersaturation and subsequent precipitation of solute particles (recrystallization step).

Since the solvent is a dilute gas after the expansion, the RESS process generates a very pure final product. Sizes and morphologies of the formed particles depend on the geometric shape of the nozzle and the initial conditions of temperature and pressure as underlined in several experimental works mainly those of Matson et al. [1], Tom et al. [2], Mohamed et al. [3], and Ksibi et al. [4].

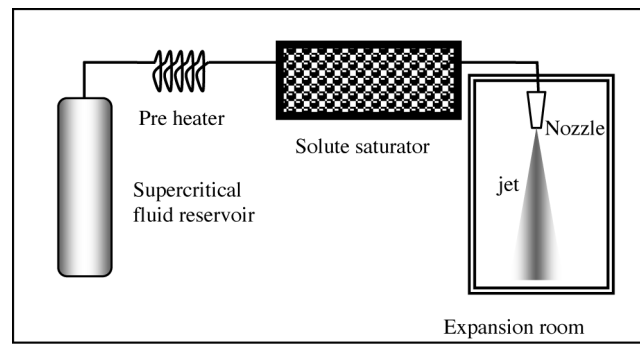


Figure 1. RESS process principle.

### 2.2 Jet and Shock Waves

It is well known that the aerodynamic study of supersonic jets exhausting from a nozzle is a problem of great importance in many industrial and aeronautical applications. For several decades, numerous experimental, numerical, and analytical investigations of the structure of supersonic jets have been undertaken [5-8], but considering very high levels of pressure is quite complicated and not yet clearly understood. Precisely, if the fluid is initially at supercritical conditions, the transition to the gas state and shock waves (Mach disc, rarefaction waves) are the main phenomena encountered in the supercritical fluid expansion as conjectured by several authors.

The imperfect matching between the downstream and the nozzle exit pressures leads to the formation of an intricate shock wave structure. Passing through the system of shock waves, the flow gradually adapts to the outlet conditions. In recent years, significant numerical progress has been achieved in understanding the fundamental aspects of the transition between regular reflection waves and Mach disc for a perfect gas flow.

### 2.3 Analysis of Anterior Numerical Works

Unfortunately, the existing experimental works on the RESS process cannot be used to elaborate an exhaustive picture about the structure of the developed flow in the expansion room, to study the variations of its characteristics or to control the particle size obtained following the expansion. All these considerations led a number of researchers to undertake the numerical simulation approach to the problem. Mathematical models aimed at a better fundamental understanding of the underlying thermo-physical phenomena, which are essential for rational design and scale-up the RESS process technology.

In recent papers, a great deal of progress has been made on the understanding of compressible Naviers-Stokes equations governing the dynamics of the SCF flow. In fact, hydrodynamic codes have been developed by treating conservation laws coupled with an equation of state representing accurately the SCF state.

Modeling for the hydrodynamics of the RESS process focused, in particular, on the flow through the nozzle, the supersonic free jet, the Mach disk, and the flow field in the expansion unit. Few measurements of temperature [9] and shadow techniques [10] showed a qualitative good agreement in general trends but did not match exactly due to the complexity of the jet control and the presence of the recrystallized particles of solute.

In general, the developed works concerning numerical simulations can be divided into two kinds of modeling: the one dimensional approach where calculation goes along the nozzle and the two dimensional approach where both nozzle and chamber expansion domains are taken into consideration.

### 2.3.1 One Dimensional Flow Modeling

In the one-dimensional approach, the contribution of several authors relies on the assumption of steady flow owing to the short residence time of the fluid inside the nozzle. The fluid, initially in a reservoir of very large dimensions, expands through a heated capillary tube of low diameter (called nozzle) and forms the free jet. This can be described by the conservation equations of mass, momentum, and energy of a compressible fluid flow. Since the diameter of the nozzle is very small, the property of the fluid at each cross section can be considered as the same, thus the approximation of one dimensional flow is reasonable. In spite of the simplifying assumptions, such model (adopted by several authors) has allowed to identify the existence of strong gradients of the various hydrodynamic variables at the time of the fluid expansion.

In the simulation by Lele et al., the adiabatic expansion of pure solvent from reservoir conditions to the exit of the capillary was analyzed [11]. The Virial equation of state for real gas, with density and temperature as independent variables has been used in the numerical flow calculations. The set of equations is as follows:

$$u \frac{d\rho}{dx} + \rho \frac{du}{dx} = 0 \quad (1)$$

$$\rho u \frac{du}{dx} + \frac{dP}{dx} = -2 \frac{fu^2\rho}{D} \quad (2)$$

$$\rho u \frac{dh}{dx} - u \frac{dP}{dx} = 2 \frac{fu^3\rho}{D} \quad (3)$$

Where  $f$  is the fanning friction factor which is proportional to shear stress at nozzle wall (it is used in momentum transfer, in general, and turbulent flow calculations in particular [12]).

In a second numerical approach, Kwauk and Debenedetti used the conservation equations of mass, the momentum and the energy to which they added a mass balance for the solid phase, resulting from the precipitation of the aqueous solution [13]. Here, the fluid is supposedly inviscid and its expansion is adiabatic and steady. It is assumed that heat effects associated with condensation and evaporation are instantaneously and uniformly distributed in the fluid phase and that there is no drag between fluid and formed particles. This mathematical model can be written as follows:

$$\frac{1}{\rho_i} \frac{d\rho_i}{dx} + \frac{1}{u} \frac{du}{dx} + \frac{1}{A} \frac{dA}{dx} = (-1)^{i+1} \delta_i \frac{J}{u\rho_i}; \quad (5)$$

$$(\sum \rho_i) u \frac{du}{dx} + \frac{dP}{dx} = 0 \quad (6)$$

$$(1 - M^2) \frac{1}{u} \frac{du}{dx} + \frac{1}{A} \frac{dA}{dx} = 0 \quad (7)$$

$$\sum \frac{\rho_i}{m_i} \frac{dh_i}{dx} + \sum \rho u \frac{du}{dx} + \frac{j(h_3 - h_2)}{um_2} = 0; \quad (8)$$

With  $\delta_i = 0$  when  $i = 1$  and  $\delta_i = 1$  otherwise ( $i = 1 \dots 3$  denotes solvent, solute and formed aerosol respectively).

These equations were solved by using an upwind differencing scheme with a second order total variation diminishing (TVD) algorithm, which can prevent oscillations of the solution.

Reverchon and Pallado proposed a one-dimensional hydrodynamic modeling of the rapid expansion of the supercritical solution through a small orifice [14]. The expansion process was subdivided into three successive steps at the nozzle inlet, along the nozzle itself, and in the expansion chamber until the Mach disc. They used the model described by equations (1-3). The Bender equation of state was associated with the conservation laws to predict thermodynamic parameters [14].

Another monodimensional hydrodynamic model has been proposed firstly by Turk [15] and then in other similar works by Helfgen et al. [16-17]. It successfully captures the vapor-liquid transition that occurs as carbon dioxide is expanded to ambient conditions. Different from the Lele et al. numerical model, this work takes into account the section area of the nozzle and the developed thermal energy which is transferred momentarily within the expansion ( $q$ ). Therefore, the conservation laws read:

$$u \frac{d\rho}{dx} + \rho \frac{du}{dx} + \frac{\rho u}{A} \frac{dA}{dx} = 0 \quad (9)$$

$$\rho u \frac{du}{dx} + \frac{dP}{dx} = -2 \frac{fu^2\rho}{D} \quad (10)$$

$$\frac{dh}{dx} + u \frac{du}{dx} = \frac{dq}{dx} \quad (11)$$

This set of equations is completed by the Bender EoS written for the carbon dioxide.

In the work of Weber et al. [18], the conservation equations of mass, momentum and energy have been written for pure solvent similarly to those of Helfgen et al. [16-17], whereas the energy conservation law (eq. 11) has been set at 0 (adiabatic evolution). They have chosen the Carnahan Starling Van Der Waals EoS to describe the thermodynamic properties of the solvent including the partial derivatives of temperature and density (Carnahan and Starling, [19]).

Finally, Hirunist et al. [20] discuss the simulation of both supercritical fluid flow inside the nozzle and its expansion at atmospheric conditions. They have taken into account only the pure supercritical solvent due to very low solute concentration along the expansion path. The used conservation laws model is identical to that of Helfgen et al. but the variation of the specific enthalpy is written as recommended by Sandler [21].

We note that this kind of models is accurately applicable in the nozzle but with difficulty in the expansion domain. Such models do not consider the existence and the propagation of different shock waves as well known in compressible fluid flows. For these reasons, other authors have developed a two dimensional numerical modeling concerning the abrupt expansion of supercritical fluid in the RESS process.

### 2.3.2 The Two Dimensional Approach

The numerical 2D simulation of the developed jet in the expansion room, in RESS process, has been firstly considered by Ksibi et al. [22-24]. The complexity of the problem lies in the capture of shock waves characterizing the structure of the supersonic jet as explained in section (2.2). These works treat simultaneously the expansion of the fluid in RESS process inside the nozzle (cylindrical tube) and in the expansion chamber in the framework of a two dimensional approach. Here, computations are done for unsteady, compressible and viscous carbon dioxide flow. Depending strongly on the pressure ratio at both the inlet and the outlet of the nozzle, this kind of flow jet appears as a succession of normal and oblique shocks. Thus, a Riemann solver based on the Roe averaging theory has to be implemented for capturing discontinuities and determining exactly different variables at the nozzle orifice such as the pressure and the velocity [25].

A numerical code has been developed by coupling the Naviers Stokes equations of the fluid flow and the Altunin and Gadestkii equation of state for carbon dioxide covering different states (SCF, liquid and gas) [26]. This code solves the full time dependent conservation laws of mass, momentum and energy for an axisymmetric flow of compressible and viscous fluid. It may be written in a conservative form as:

$$\frac{\partial U}{\partial t} + \frac{\partial(F(U))}{\partial r} + \frac{\partial(G(U))}{\partial z} + \frac{H(U)}{r} = 0 \quad (12)$$

Where  $U$  is the solution vector of the conservative terms and  $F$  and  $G$  are fluxes in both directions including the Euler part and the dissipating terms. They are written as:

$$U = \begin{pmatrix} \rho \\ \rho u \\ \rho w \\ \rho E \end{pmatrix}; \quad F = \begin{pmatrix} \rho u \\ \rho u^2 + P + \tau_{rr} \\ \rho uw + \tau_{rz} \\ (\rho E + P)u + u\tau_{rr} + w\tau_{rz} + \kappa \frac{\partial T}{\partial r} \end{pmatrix} \quad (13)$$

$$G = \begin{pmatrix} \rho w \\ \rho uw + \tau_{rz} \\ \rho w^2 + P + \tau_{zz} \\ (\rho E + P)w + u\tau_{rz} + w\tau_{zz} + \kappa \frac{\partial T}{\partial z} \end{pmatrix}; \quad \text{and} \quad H = \begin{pmatrix} \rho u \\ \rho u^2 \\ \rho uw \\ (\rho E + P)u + u\tau_{rr} + w\tau_{rz} + \kappa \frac{\partial T}{\partial r} \end{pmatrix}$$

Where the dissipation tensor  $\tau$  is expressed by

$$\begin{cases} \tau_{rr} = \frac{2}{3}\mu \left( 2\frac{\partial w}{\partial r} - \frac{\partial u}{\partial z} \right) \\ \tau_{zz} = \frac{2}{3}\mu \left( 2\frac{\partial u}{\partial z} - \frac{\partial w}{\partial r} \right) \\ \tau_{rz} = \mu \left( \frac{\partial u}{\partial r} + \frac{\partial w}{\partial z} \right) \end{cases} \quad (14)$$

This set of equations has been solved by using the Total Variation Diminishing algorithm (TVD) [27]. The convergence was accelerated by an implicit linearisation using the altering direction implicit (ADI) formulation.

More recently, Khalil et al. have carried out a numerical simulation of the expansion of instationnary and axisymmetric flow of supercritical fluid through a cylindrical section orifice [10]. They have studied the interaction between the jet and the plate of deposition for the case of an adiabatic expansion of carbon dioxide under its supercritical state.

The time dependent partial differential equations to be solved for inviscid free jet supersonic expansion are given in conservation form as follows:

$$\frac{\partial E}{\partial t} + \frac{\partial F}{\partial x} + \frac{\partial G}{\partial r} + \frac{H}{r} = 0 \quad (15)$$

Where

$$E = \begin{pmatrix} \rho \\ \rho u \\ \rho w \\ \rho \left| I + \frac{1}{2}(w^2 + v^2) \right| \end{pmatrix}; \quad F = \begin{pmatrix} \rho u \\ \rho u^2 + P \\ \rho uw \\ \left( \rho \left| I + \frac{1}{2}(u^2 + w^2) \right| + P \right) u \end{pmatrix} \quad (16)$$

$$G = \begin{pmatrix} \rho w \\ \rho u w \\ \rho w^2 + P \\ \left( \rho \left| I + \frac{1}{2}(u^2 + w^2) \right| + P \right) w \end{pmatrix}; \text{ and } H = \begin{pmatrix} \rho w \\ \rho u w \\ \rho w^2 \\ \left( \rho \left| I + \frac{1}{2}(u^2 + w^2) \right| + P \right) w \end{pmatrix} \quad (16)$$

A full time step has been used in the predictor step with forward differencing and an artificial numerical viscosity has been incorporated as suggested by Anderson [7].

In 2005, Ben Moussa et al. have published their work focused on the hydrodynamic simulation of the RESS process with different nozzle shapes and designs [28-29]. The numerical model is basically the one developed by Ksibi et al. improved by treating the inlet conditions and the optimization of the flow rate [22]. The governing transport equations involving the hydrodynamic field have been solved using the finite volume method. In particular, the grid took in account the structure of the developed jet. So, curved meshes were chosen and calculus implementation was transformed from the Cartesian system to the curvilinear one. Due to the enormous difference in scale between nozzle dimensions and those of the precipitation unit, refining meshing techniques were also used. The nozzle has different shapes for which the exit radius varies between 40 and 200  $\mu\text{m}$ s. The time step is conditioned by the Courant Frederic Levy (CFL) number.

At the beginning of the calculation, the time step was set at  $10^{-9}$  s. The established algorithm causes the time step to automatically increase when flow instabilities are minor. The numerical simulations are achieved when a stationary configuration of the flow is obtained.

### 3. COMPARISON OF RESULTS AND DISCUSSIONS

The preceding models incorporate the essential physics of the solvent expansion in the RESS process without considering, however, the solute presence. Thus, this is the natural starting point when trying to understand the basic trends that relate particle size and process conditions in RESS. Numerical calculations given by several authors and summarized in table (1) are useful for uncovering basic trends, more than they are in predicting exact quantities of different hydrodynamic variables. Indeed, the developed codes give profiles of different thermodynamic and kinetic parameters in the capillary nozzle and the jet. The calculation of these gradients locates in some way the supersaturation region in the nozzle where nucleation can occur and relate it to the capillary dimensions and geometry, table (2).

As a common feature, results of flow field calculation show a strong change of all parameters in the expansion region, whereas inside the capillary nozzle the change is moderate. At the nozzle exit the sound speed is exceeded and the flow expands further in a supersonic free jet when the flat plate is placed faraway from the nozzle. Here, the rate of change is extremely fast and separation of the solute is induced systematically. When the supercritical fluid exits the nozzle orifice at Mach one or faster, it speeds up, expands, and as the pressure drops, it enters a regime where the EoS becomes concave [30].

To illustrate such behaviors, hereafter, the density, the velocity, etc along the capillary nozzle and the expansion room are made dimensionless by dividing them with the inlet values. Indeed, each dimensionless variable is equal to the unity at the inlet nozzle ( $X = 0$ ). The capillary nozzle outlet coordinate is equal to  $X = 1$ . Similarly, in the expansion room the orifice exit is located at  $X = 0$  and the plate position is equal to  $X = 1$  as required in the dimensionless analysis.

#### 3.1 Flow Fields in the Nozzle

As explained before, to identify the probable location of phase separation of recrystallized solute, the adiabatic expansion of the pure solvent from tank conditions to the exit of the capillary has been analyzed by several authors. Lele and Shine [11] reported that the solution expansion during RESS takes place at the orifice inlet, i.e., inside the capillary nozzle.

Figure (2) shows the dimensionless density variations of the supercritical fluid along the capillary axis as obtained by several authors. Here, we consider that capillary nozzles are cylindrical pipes with an inner diameter of many tens of micrometers (see table 2). Concerning the dimensionless density

**Table 1: Resumed numerical simulation works of the supercritical fluid expansion**

	Conservation Laws	Dissipation	Computation Domain	Fluid EOS	Numerical Methods
Lele et al (1992)	1-dimensional, Isentropic, Stationnary.	Fanning friction Factor	Nozzle	Altunin EOS	<ul style="list-style-type: none"> <li>Finite difference</li> <li>Regular grid</li> </ul>
Kwauk et al (1993)	1-dimensional, Isentropic, Stationnary	None	Nozzle	Peng Robinson EOS	<ul style="list-style-type: none"> <li>Finite difference</li> <li>TVD algorithm</li> </ul>
Ksibi et al (1995-2006)	2-dimensional, Instationnary, Axisymmetric, Full Naviers Stokes equations	Stress tensor for newtonian fluid	Nozzle + Expansion room	Altunin and Gadestkii EOS	<ul style="list-style-type: none"> <li>Finite difference</li> <li>TVD algorithm</li> <li>Irregular grid</li> <li>Shock capture: Roe averaged technique for real gases</li> </ul>
Reverchon et al (1996)	1-dimensional, Isentropic, Stationnary.	Fanning friction factor	Nozzle + Expansion room (until the Mach disk)	Bender EOS	<ul style="list-style-type: none"> <li>Finite difference</li> </ul>
Turk (1999) + Helfgen et al. (2001-2003)	1-dimensional, Stationnary.	Fanning friction factor	Nozzle	Bender EOS	<ul style="list-style-type: none"> <li>Finite difference</li> <li>Shock capture: Stromfadentheorie (Streamline theory)</li> </ul>
Weber et al (2001)	1-dimensional, Isentropic, Stationnary.	Fanning friction factor	Nozzle	Carnahan-Straling VDW EOS	<ul style="list-style-type: none"> <li>Finite difference</li> </ul>
Khalil et al (2003)	2-dimensional, Instationnary, Axisymmetric, Full Euler equations	Inviscid fluid	Expansion room	Redlich Kwong EOS	<ul style="list-style-type: none"> <li>Finite difference</li> <li>Numerical viscosity</li> </ul>
Hurnist et al. (2004)	1-dimensional, Stationnary.	Fanning friction factor	Nozzle + Expansion room	Extended Bender EOS	<ul style="list-style-type: none"> <li>Finite difference</li> </ul>
Ben Moussa et al (2005)	2-dimensional, Instationnary, Axisymmetric, Full Naviers Stokes equations	Stress tensor for newtonian fluid	Different nozzle geometries + Expansion room	Altunin and Gadestkii EOS	<ul style="list-style-type: none"> <li>Finite difference</li> <li>TVD algorithm</li> <li>Curvilinear and irregular grid</li> <li>Shock capture: Roe averaged technique for real gases</li> </ul>

**Table 2: Nozzle dimensions and internal geometry**

Authors/ Nozzle	Nozzle Geometry	Diameter ( $10^{-6}$ m)	Length ( $10^{-3}$ m)
Kwauk et al.	Convergent	20–30	10
Lele et al.	Cylindrical	30	0,255
Ksibi et al.	Cylindrical	110	10
Weber et al.	Convergent-Cylindrical	100	0,1
Reverchon et al.	Cylindrical	40	0,8
Helfgen et al.	Cylindrical	50	0,05
Ben Moussa et al.	<ul style="list-style-type: none"> <li>• Cylindrical</li> <li>• Convergent</li> <li>• Divergent-convergent</li> <li>• Cylindrical with shrinking</li> </ul>	40–220	1–15
Hirunsit et al.	Cylindrical	50	1–2

profile calculated by Lele et al. [11], we note that the abrupt falling of the density at the capillary inlet may be due to non appropriate boundary conditions. For the other calculations, the density profile decreases slightly along the capillary tube [31].

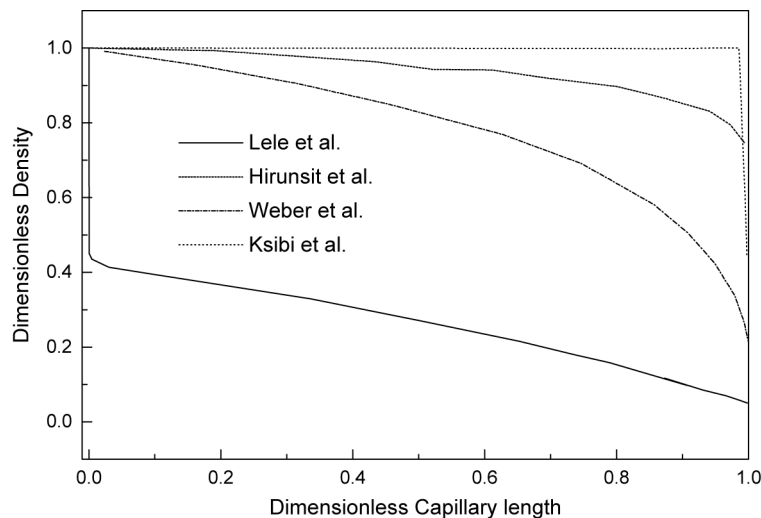


Figure 2. Comparison of the dimensionless density profile along the capillary nozzle calculated by several authors.

In recent numerical simulations such as that of Ben Moussa et al. [28], the density profile in the capillary nozzle maintains its inlet value until the exit orifice where rarefaction waves are located.

Improvement of calculations inside the capillary nozzle has been obtained by considering a two dimensional flow and an accurate formulation of the inlet/outlet boundary conditions of the problem. There exists an intensive expansion which generates an instantaneous adiabatic and irreversible evolution. Under these conditions, the major part of pressure and density drops is due to the friction rather than the kinetic effect. This can be seen from a very small vertical drop of the density profile inside the nozzle before the exit orifice.

Figure (3) shows the dimensionless temperature profiles along the nozzle, corresponding to several published works. We notice that the initial temperature decreases along the nozzle in some cases due to the simplified assumptions as the adiabatic evolution and the constant friction factor. The calculated temperature along the nozzle in the case of Kwauk and Debenedetti [13] shows an important gradient of temperature located inside the nozzle. Accordingly, the fluid expansion and its separation from the solute can occur in the nozzle. This case is always avoided in experimental works to keep away from the orifice plugging.

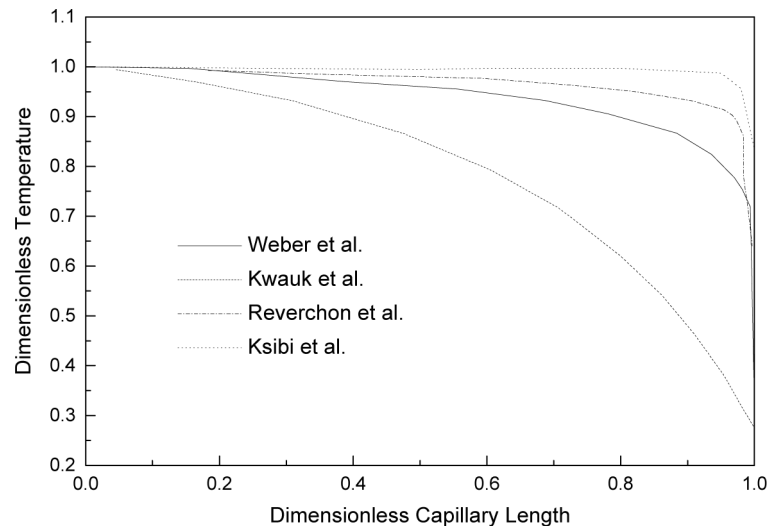


Figure 3. Comparison of the dimensionless temperature profile along the capillary nozzle.

Other profiles depicted in figure (3) show accurately the temperature variation along the nozzle. We notice that this variable maintains theoretically its value until the orifice exit for a low viscous fluid as supercritical carbon dioxide. This agrees qualitatively with the numerical studies of compressible ideal gas expansions through a cylindrical nozzle.

Figure (4) shows the evolution of the Mach number for carbon dioxide expanding along the capillary axis. We notice that inlet fluid velocity in the case of Weber et al. simulation is initialized at very low level, therefore the Mach number is quite small at the nozzle inlet when the inner geometry of the nozzle is cylindrical.

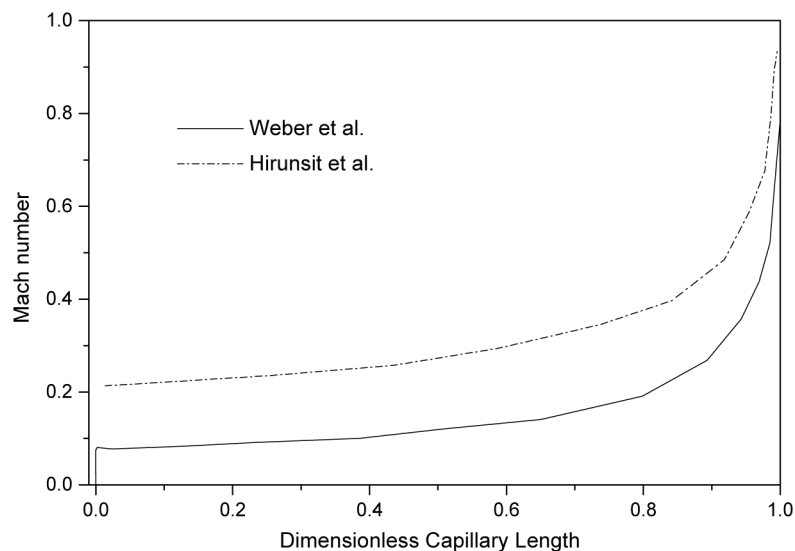


Figure 4. Comparison of the Mach number profile along the capillary nozzle.

Moreover, along the capillary nozzle, the Mach number is set at a low value for subsonic calculation cases. Very close to the nozzle exit the latter increases abruptly to reach the unity and therefore the sonic regime. When the fluid expands at the nozzle exit, the free supersonic jet is formed and the velocity increases rapidly until it reaches the Mach disc where the maximum velocity exceeds 500 m/s as mentioned by several authors mainly Hirunsit et al. [22], and Ksibi et al. [22].

We have varied the capillary nozzle dimensions by altering their length and inner diameter for the same numerical configuration [24]. A new dimensionless parameter is defined as the ratio of the inlet gap pressure and the outlet one, and given as a function of the nozzle dimensions, Ben Moussa et al. [28].

Here, it is underlined that favorable nucleation and coagulation conditions can be computed using the obtained hydrodynamic fields.

The nozzle shape effect, on the RESS process hydrodynamics, has been considered by varying the inner geometry while keeping the supercritical inlet conditions as explained by Ben Moussa et al. [28]. Thus, three types of inner nozzle shape are treated numerically: cylindrical nozzle, convergent nozzle and cylindrical nozzle with shrinking, figure (5). In these different cases, simulations of the dimensionless density along the nozzle axis shows that a pronounced decrease of this variable can be obtained inside the nozzle when the inlet fluid flow is subsonic in figure (6). As a result, higher supersaturation of the considered supercritical solution ratios can occur before the nozzle exit. Inside the cylindrical nozzle with shrinking, a fall of the density can exceed 80 % of the inlet density value. Nevertheless, the behavior of the fluid flow is quite the same at the nozzle orifice for all geometries. The fluid velocity can be altered inside the nozzle when its inner shape is varied. The Mach number increases at the contracted section of the nozzle when the fluid flow is initially subsonic. Its value joins exactly that of the cylindrical case, very close the orifice exit in figure (7).

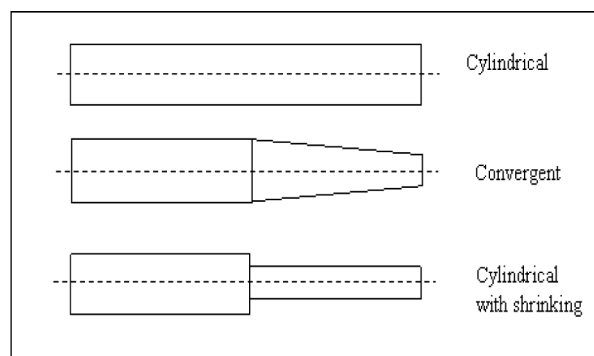


Figure 5. Different nozzle shapes.

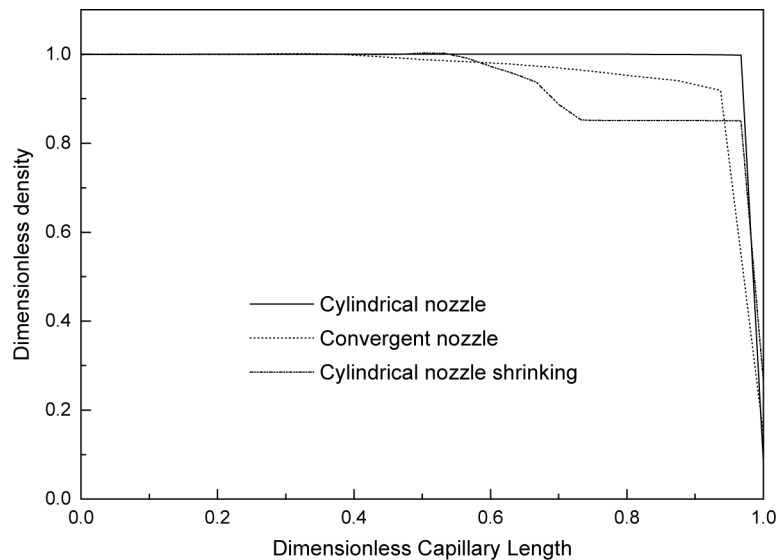


Figure 6. Comparison of the dimensionless density profile along different nozzle shapes using curvilinear grid model of Ben Moussa et al. (2005).

### 3.2 Flow Field in the Expansion Chamber

It is clear that the significant effect of a supercritical fluid expansion to a low pressure level is the obtaining of a very low temperature downstream as expected by several authors. The temperature is a serious issue for clustering and growth in RESS experiments since the solute solubility is very sensitive to this parameter. In the expansion chamber the separation is induced when the velocity increases

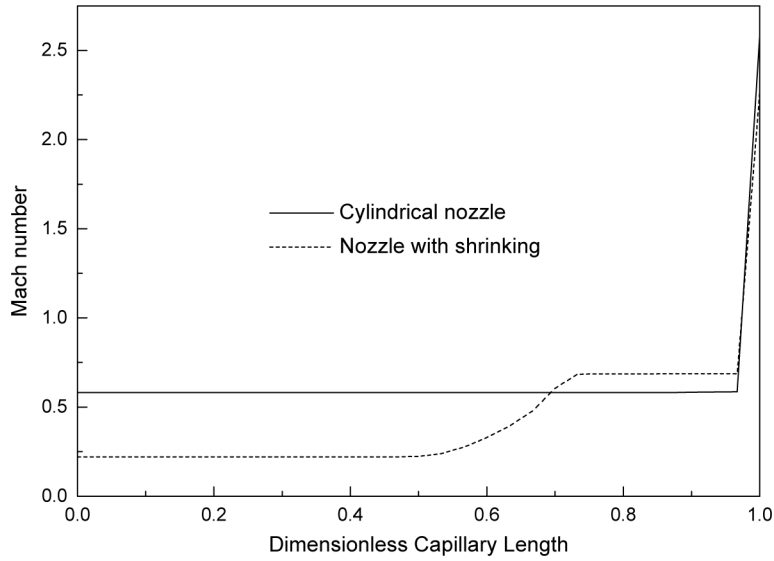


Figure 7. Comparison of the Mach number profile along different nozzle shapes using curvilinear grid model of Ben Moussa et al. (2005).

extremely due to the pressure, temperature, and density abrupt fallings. Interestingly, the ideal gas approximation is reasonable as first approximation for the shock location and pressure profiles in the expansion. Nevertheless, thermodynamic variables are implemented inaccurately close to the orifice and before the Mach disc.

Supersonic free jet pressure and temperature are highly reduced, and therefore, the density decreases over several orders of magnitude as can be seen in figures (8 and 9). The decrease of density and temperature lead to solvent condensation depending on the preexpansion conditions. The shape of the supersonic free jet is supposed to be conical and a linear increase of the jet diameter along the expansion can be assumed, Hirunsit et al. [20]. Nevertheless, we highlight the increase of dimensionless density in the expansion chamber when crossing the Mach disc and that is due to calculations made without a shock capture scheme, figure (8).

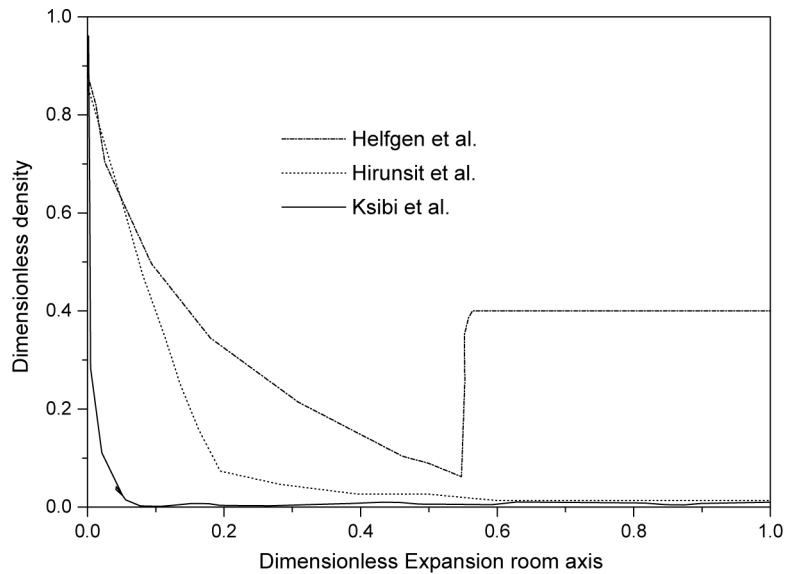


Figure 8. Comparison of the temperature profile a long the expansion room axis.

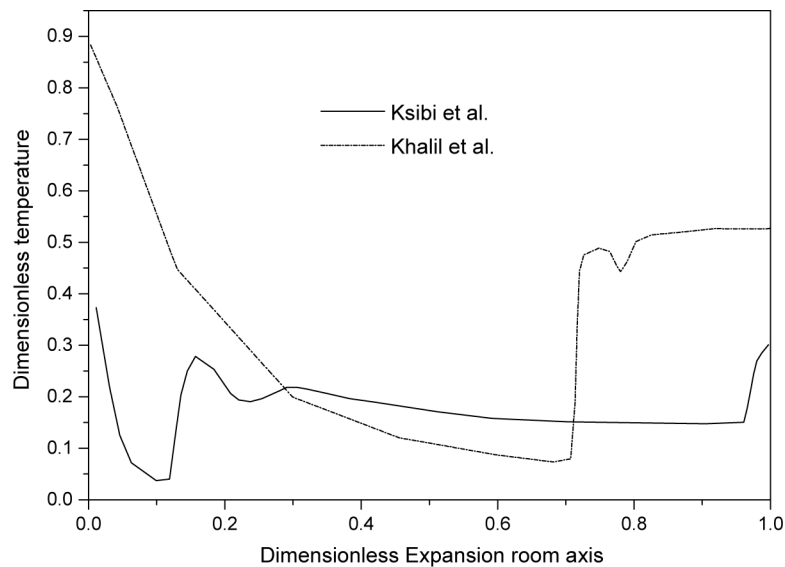


Figure 9. Comparison of the temperature profile along the expansion room axis.

After the nozzle exit, the pressure continues to decrease until it reaches the ambient pressure. However, the temperature decrease ends at minimum dimensionless value of approximately 0.2, which is a few millimeters away from the nozzle exit. After that point, the temperature tends to increase as a result of the heat exchange with the surrounding. The rapid decrease of both temperature and pressure, occurring at the transition from the nozzle exit to the free jet region, results in a sharp drop of the fluid density as detailed before. Then it continues to decrease gradually till it levels off, probably due to the picking-up of temperature as noted by Hirunsit et al. [20].

By considering only the Euler flux, Khalil et al. [10] have found that the Mach disc and flow properties are more accurately defined by including a numerical viscosity. They notice that the oscillations persist downstream of the shock, an amalgam between accuracy and the dampening of the numerical oscillations.

By taking into account shock waves in the jet, the expansion induces an abrupt fall of the thermodynamic parameters like the temperature (laminated medium). Very low values are reached (about 20 %) and oscillations are captured due to the presence of rarefaction waves and the Mach disc. Concerning the thermal behavior at the plate, we note a very thick thermal boundary layer in the case of the work by Khalil et al. [10] which cannot reflect the very cold jet impacting. In the case of Ksibi et al. [22] temperature profile, we notice the capture of the Mach disc where the temperature should increase and oscillate along the jet until the jet impacts the frontal plate. There, a thin boundary layer is localized and elevation of temperature at this zone leads to an increase.

In the expansion room, speed increases continuously to the plate without being deteriorated by the presence of the rarefaction waves, figure (10). The Mach disc is moved away to a more significant distance from the nozzle exit, i.e. the case of an expansion in a very low pressure medium (about 100 KPa) as studied by Ksibi et al. [22]. Recent calculations are implemented within a stagnated compressed gas (many tens of bars) in the expansion room to show the importance of the pressure outlet on the formed jet and then on the particle transport, Ksibi et al. [29]. These calculation cases lead to a better control of the jet size and thereafter to prevent the collision of particles, reduce their sizes, and disfavor the formation of the aggregates.

#### 4. CONCLUSION

CFD simulations have been performed for the rapid expansion of a supercritical fluid by several authors using different forms of conservation laws and related assumptions.

In the present work comparison of different hydrodynamic codes has been undertaken by analyzing different assumptions, the used equations of state and shock capture techniques. The majority of analyzed works treat the Naviers-Stokes equations coupled with an accurate equation of state for one-dimensional and stationary flow.

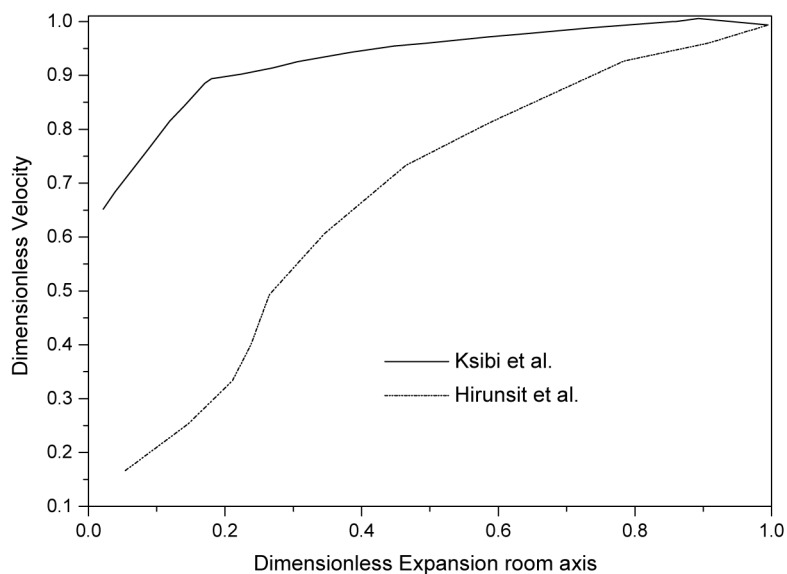


Figure 10. Comparison of the velocity profile along the expansion room axis.

More recently, several papers have reconsidered this problem by extending the current one-dimensional model to a two-dimensional grid. Here, a Riemann solver based on the Roe theory is implemented for capturing discontinuities. Therefore, such approach makes it possible to avoid nozzle plugging in RESS process by choosing the optimal nozzle dimensions and thermodynamic operating parameters.

The high value of the pre/post-expansion pressures ratio ( $P_{in}/P_{out}$ ) involves surely a flow jet accompanied by several right and oblique shocks as the Mach disc. Therefore, the consideration of non-stationary flow and a shock capture scheme are required. The rapid decreases of both temperature and pressure, occurring at the transition from the nozzle exit to the free jet region, results in a sharp drop of the fluid density as shown in different analyzed works.

Furthermore, the effects of pre/post-expansion pressure and temperature and the nozzle dimensions on the fluid flow have been examined. The results show that the variation of these parameters may lead to supersaturation increase at the cylindrical nozzle exit and a simultaneous separation of the solute from the expanded solvent. For other inner nozzle shapes such as the convergent one, simulations show how the super-saturation region can be moved in the nozzle.

## 5. REFERENCES

1. Matson, D.W., Fulton, J.L., Petersen, R.C., Smith, R.D., Rapid expansion of supercritical fluid solutions: solute formation of powders, thin films and fibers, *Industrial and Engineering Chemistry Research*, 1987, 26, 2298–2306.
2. Tom, J.W., Debenedetti, P.G., Jerome, R., Precipitation of poly(L-lactic acid) and composite poly(L-lactic acid)- pyrene particles by rapid expansion of supercritical solutions, *Journal of Supercritical Fluids*, 1994, 7, 9–29.
3. Mohamed, R.S., Debenedetti, P.G., Prud'homme, R.K., Effects of process conditions on crystals obtained from superoxide mixtures, *AIChE Journal*, 1989, 35, 325–328.
4. Ksibi, H. Subra, P. Garrabos, Y., Formation of fine powders of caffeine by the RESS process, *Advanced Powder Technology*, 1995, 6(1), 25–33.
5. Courant, R., Friedrichs, K.O., *Supersonic Flow and Shock Waves*, Interscience Publishers Inc., New York, 1948.
6. Ashkenas H., Sherman F.S., The structure and utilization of supersonic free jets in low density wind tunnels. in: H.L. Dryden, T. von Karman (Eds.), *Advances in Applied Mechanics*, Suppl. 3, in: J.H. de Leeuw (Ed.), *Rarefied Gas Dynamics*, vol. 2, 84–105, 1965.
7. Anderson, J.D., A Time dependent analysis for vibrational and chemical nonequilibrium nozzle flows. *AIAA Journal*, 1970, 8, 545–550.
8. Campargue R., Progress in over expanded supersonic jets and skimmed molecular beams in free-jet zones of silence. *Journal of Physical Chemistry*. , 1984, 88 (20) 4466–4474.

9. Reverchon, E., Pallado, P., Hydrodynamic modeling of the RESS process, *Journal of Supercritical Fluids*, 1995, 8 (4), 318–328.
10. Khalil I., Miller, D.R., The Structure of Supercritical Fluid Free-Jet Expansions; *AIChE Journal*, 2004, 50 (11), 2697–2704.
11. Lele A.K., Shine, A.D., Morphology of Polymers Precipitated from a Supercritical Solvent, *AIChE Journal*, 1992, 38, 742.
12. Musschenga, E.E., Hamersma, P.J., Fortuin, J.M.H., Momentum, heat and mass transfer in turbulent pipe flow. The extended random surface renewal model, *Chemical Engineering Science*, 1992, 47 (17-18), 4373–4392.
13. Kwauk, X., Debenedetti, P.G., Mathematical modeling of aerosol formation by rapid expansion of supercritical solutions in a converging nozzle, *Journal of Aerosol Science*, 1993, 24 (4), 445–469.
14. Bender, E., Equation of State Exactly Representing the Phase Behavior of Pure Substances, *Proceedings of the 5<sup>th</sup> Symp. on Thermophysical Properties*, ASME, New York, 1970, 227.
15. Türk, M., (1999). Formation of Small Organic Particles by RESS: Experimental and Theoretical Investigations, *Journal of Supercritical Fluids*, 15, 79.
16. Helfgen, B., Hils, P., Holzknacht, Ch., Türk, M., Schaber K., Simulation of particle formation during the rapid expansion of supercritical solutions, *Journal of Aerosol Science*, 2001, 32, 295–319.
17. Helfgen, B., Turk, M., Schaber K., Hydrodynamic and aerosol modelling of the rapid expansion of supercritical solutions (RESS-process). *Journal of Supercritical Fluids*, 2003, 26, 225–242.
18. Weber, M. Russell, L.M. Debenedetti, P.G., Mathematical modeling of nucleation and growth of particles formed by the rapid expansion of a supercritical solution under subsonic conditions; *Journal of Supercritical Fluids*, 2002, 23, 65–80.
19. Carnahan, N.F., Starling, K.E., Intermolecular repulsions and the equation of state for fluids, *AIChE Journal*, 1972, 18 (6), 1184–1189.
20. Hirunsit, P., Huang, Z., Srinophakun, T., Charoenchaitrakool, M., Kawi, S., Particle formation of ibuprofen–supercritical CO<sub>2</sub> system from rapid expansion of supercritical solutions (RESS): A mathematical model; *Powder Technology*, 2005, 154, 83–94.
21. Sandler S.I., *Chemical and Engineering Thermodynamics*. New York: John Wiley & Sons, Inc, 1999.
22. Ksibi, H., Tenaud, C., Subra, P., Garrabos, Y., Numerical Simulation of the rapid expansion of supercritical fluid flow, *European Journal of Mechanics /B Fluids*, 1996, 15(4), 569–596.
23. Ksibi, H., Influence of the capillary dimensions in RESS process, *Chem. and Biochem. Eng. Quarterly Journal*, 1999, 13 (3), 139–144.
24. Ksibi, H., Effect of Small Capillaries on the Hydrodynamic Conditions in the RESS Process, *Proceedings of the 5<sup>th</sup> Meeting on Supercritical Fluids; Materials and Natural Products processing*, M. Perrut and P. Subra (Eds.), Tome 1: Materials, Nice, 1998, 319–324.
25. Roe, P.L., Approximate Riemann solvers, parameter vectors and difference schemes, *Journal of Comput. Phys.*, 1981, 43, 357–372.
26. Altunin, V.V., Gadetskii, O.G., Method of formulating the fundamental equations of state for pure substances from varied experimental data, *Teplofizika Vysokikh Temperatur* 1971, 9 (3), 527–534
27. Harten, A., Yee, H.C., Implicit TVD schemes for hyperbolic conservation laws in curvilinear coordinates, *AIAA Journal*, 1986, 25, 266–274.
28. Ben Moussa, A., Ksibi, H., Tenaud, C., Baccar, M., Paramètres géométriques de contrôle de la détente d'un fluide supercritique, *International Journal of Thermal Sciences*, 2005, 44, 774–786.
29. Ksibi, H., Ben Moussa, A., Baccar, M., Powder structure transition under the recrystallization conditions in the RESS Process, *Chemical Engineering & Technology*, 2006, 29 (7), 868–874.
30. Chitanvis, S.M., Initiation of rapidly expanding supercritical fluids, *Physica A*, 2003, 322, 55–72.
31. Weber, M. Thies, M.C. A simplified and generalized model for the rapid expansion of supercritical solutions; *Journal of Supercritical Fluids*, 2007, 40 (3), 402–419.